Power Line Fault Detection Combining Deep Learning and Digital Twin Model

Siyu Wu[1]*, Xin Yan[2]
Zhengzhou Vocational University of Information and Technology, Zhenzhou 450008, China[1]
Yellow River Engineering Consulting Co., Ltd., Zhengzhou 450003, China[2]

***Abstract*—To address the issue of inadequate diagnosis of power line faults, an automated power line fault diagnosis technology is put forward. In this context, the research leverages the object detection algorithm YOLOv5 to construct a fault diagnosis model and enhances its anchor box loss function. In addition, the study introduces digital twin models for fault point localization, and improves the recognition model by introducing GhostNet and attention mechanism, thereby enhancing the diagnostic performance of the technology in multi-objective scenarios. In the performance test of the loss function, the improved loss function performs the best in both regression loss and intersection over union ratio, with the average loss value and intersection over union ratio being 125 and 0.986, respectively. In multi-scenario fault diagnosis, the research model performs the best in accuracy and model loss, with values of 0.986 and 0.00125, respectively. In multi-scenario fault diagnosis, such as abnormal heating detection, when the number of targets is 4, the relative error of the research model is 0.86%, which is better than similar models. Finally, in the testing of frame rate recognition and diagnostic time, the research model shows excellent performance, surpassing similar technologies. The technology proposed by the research has good application effects. This study provides technical support for the construction of power informatization and line maintenance.**

Keywords*—YOLOv5; route; fault diagnosis; digital twin; loss function

I. Introduction

As a key component of the power system, the safe and stable operation of power lines is crucial for socio-economic development. However, the environment in which power lines are located is complex and ever-changing, and they are susceptible to natural disasters, human damage, and other factors, leading to frequent failures. Traditional power line fault detection methods mainly rely on manual inspection and rule-based signal processing, which are inefficient, costly, and difficult to cope with complex and changing fault modes. In recent years, with the development of artificial intelligence technology, Deep Learning (DL) has gradually been applied in the field of power line fault detection and has achieved excellent results. For example, fault diagnosis technology based on deep convolutional neural networks can capture key features of power lines and train to recognize complex targets. In addition, there is a fault diagnosis technology based on recurrent neural networks, which achieves fault analysis through feature extraction of power lines. However, the above-mentioned DL techniques still face problems in the processing of power lines in complex scenarios, such as high cost of data annotation, long model training time, and poor recognition accuracy. In recent years, You Only Look Once version 5 (YOLOv5), as an advanced object detection algorithm, has shown great potential in power line fault detection due to its fast detection speed and high accuracy. Compared to traditional convolutional neural networks, it can handle more complex background environments and detect a larger range of targets. However, it still faces difficulties in dealing with small targets and complex scenarios, and precise positioning of fault areas is also challenging. At present, digital twin (DT) models are gradually receiving attention in the field of electricity. DTs can reflect the state and behavior of physical systems in real time by constructing virtual models that correspond to physical entities. They use data collected by sensors to analyze the operating status of power lines, thereby more accurately locating fault points. Consequently, to achieve efficient detection of power faults, the research has introduced an intelligent line fault diagnosis technology that integrates DT models with target-detection algorithms, specifically YOLOv5. This technology boasts two notable innovations. Firstly, it focuses on optimizing the anchor box loss function. By doing so, it can effectively filter out irrelevant targets, thereby streamlining the diagnosis process and enhancing overall efficiency. Secondly, the research incorporates the GhostNet architecture and the Coordinate Attention (CA) mechanism into the YOLOv5 algorithm. This integration aims to refine the algorithm's capabilities, enabling it to deliver superior diagnostic performance even in complex operational scenarios. In summary, this study offers crucial technical support for the establishment of a stable and secure power system.

This study is divided into six sections. The first section is the introduction, which analyzes the shortcomings of traditional power line detection methods and the application prospects of DL and DT technology. The second section is related work, which summarizes the current related research. The third section is the methodology section, which proposes a fault detection technique based on improved YOLOv5 and DT model, including optimizing the anchor box loss function, introducing GhostNet and CA mechanism, etc. The forth section is the analysis of experimental results, which verifies the performance advantages of improved loss functions (such as Focal IoU), and compares the accuracy, loss values, frame rates, and diagnostic time of different models in multi scenario fault detection. The fifth section is a discussion of the results, demonstrating the efficiency and superiority of the research model in fault detection. The sixth section is the conclusion of the study.

II. Related Work

Ensuring the secure and dependable functioning of power grid lines is essential for reliable power supply. Traditional detection methods rely on manual inspection, which suffers from issues like inefficiency and poor real-time performance [1]. The rise of DL technology has offered an alternative methodology for power grid line detection. It constructs a complex neural network model to automatically extract multi-source data features such as images and signals, achieving efficient identification and localization of line faults [2]. Alexander Stonier et al. carried out a study on the problem of faults in solar photovoltaic microgrids. To improve the effectiveness of fault detection, it analyzed common faults in photovoltaic modules, inverters, batteries, and charging controllers. Techniques such as DL were introduced to analyze and classify fault types. The research results indicated that this technology could effectively detect fault problems. It provided strategies for the continuous operation of microgrids under fault conditions, but its shortcomings lied in insufficient depth in analysis of the implementation details of specific diagnostic techniques [3]. Shakiba et al. carried out study on the issue of insufficient fault detection in transmission lines. So research was conducted on machine learning-based transmission line fault detection technology, covering traditional methods such as Naive Bayes classifiers. A detection model was constructed using deep convolutional networks and fuzzy neural networks, and fault diagnosis was achieved through adaptive inference and other methods. The findings indicated that this study could significantly improve the accuracy of line detection and meet the safety requirements of the power grid. However, its shortcomings lied in the lack of in-depth validation of the model's generalization ability [4]. Li et al. studied the issue of insufficient accuracy in unmanned aerial vehicle (UAV) power inspection systems and designed a detection system based on intelligent UAVs. The technical process included autonomous planning of detection paths, sliding mode control algorithms, and motion detection schemes, which used advanced object detection algorithms to achieve problem analysis. The research results indicated that the system significantly enhanced the effectiveness and precision of power inspection, but its shortcomings lied in the need to further improve the endurance and flight stability of UAVs in complex environments [5]. Chen et al. studied the problem of insufficient diagnosis of intelligent distribution live working robots and proposed an intelligent distribution live working robot system based on stereo cameras to replace manual completion of high-risk distribution network maintenance tasks. This system combined dual robotic arms, wireless tools, visual perception systems, and path planning technology in virtual simulation environments. The research results indicated that technology could achieve problem diagnosis within a brief timeframe with higher efficiency. However, the technical limitation lied in its limited adaptability to complex job scenarios [6].

As the power system undergoes expansion and grows increasingly complex, conventional approaches to power fault detection are encountering numerous challenges. DT technology achieves precise monitoring and fault warning of power equipment by constructing virtual models and real-time mapping of physical entity states. Gómez Luna et al. conducted research on overcurrent protection caused by distributed energy access in distribution networks and proposed a new overcurrent protection scheme based on DTs. This scheme adopted coordinated protection standard settings and coordinated intelligent electronic devices, utilizing power hardware technology to connect real relays to the DT model of the analog network. The outcomes revealed that this method improved the coordination and adaptability of overcurrent protection, but there is still a problem of lack of coordination with different distributed energy sources [7]. Sinagra et al. conducted research on pressure regulation and energy recovery in water distribution networks and proposed an advanced real-time control logic based on DTs. This technology optimized the configuration of turbines and valves, dynamically updated network status using DT models, and achieved efficient hydroelectric power generation. The results indicated that this technology exhibited higher robustness and efficiency in different operational scenarios, but its adaptability to complex networks still needs further validation [8]. Sharma et al. conducted research on the bottleneck problem of electric vehicle battery assembly and proposed a three-stage DT design and analysis approach. This method developed robot assembly line configurations of different scales through DT design and simulation, and evaluated and optimized the speed and cost of the assembly system. The research results indicated that this method could quickly and economically assemble electric vehicle battery modules, but the implementation difficulty and cost control in actual production still need further exploration [9].

In summary, equipment failures in the power system will pose specific challenges to the operation and safety of the power grid. Currently, DL finds extensive application in the domain of power safety, providing technical support for power safety data analysis and fault diagnosis. In addition, DT technology adopts a physical virtual construction of power detection system, which can analyze the power grid status in real time and provide support for power system equipment failures. Therefore, to address the issues of slow and poor accuracy in current power line fault diagnosis, an intelligent line fault diagnosis technology is proposed by combining DT model and YOLOv5 algorithm.

III. Methods and Materials

A. Modeling of Power Line Fault Detection Based on DL

With the expansion of the power system, frequent line failures seriously affect the reliability of power supply. Traditional detection approaches have low efficiency and poor accuracy, making it hard to fulfill the requirements. Therefore, the research proposes an intelligent line fault detection technology based on improved YOLOv5 to enhance the safety operation of the power grid. The YOLOv5 network structure is in Fig. 1.

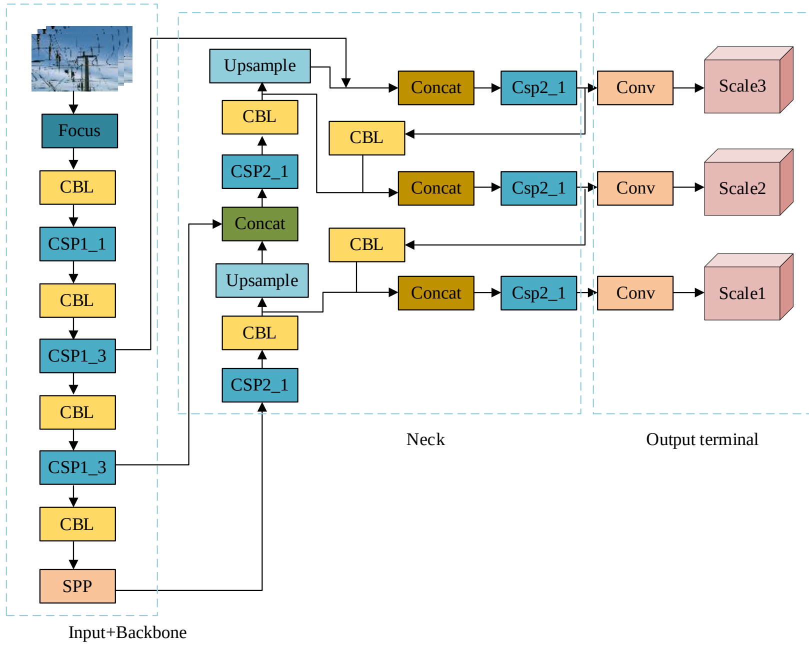

Fig. 1. YOLOv5 network structure.

According to Fig. 1, YOLOv5 mainly consists of input terminals, backbone, neck, and output terminals [10]. Among them, the input terminal inputs the power line image data that needs to be detected (collected by the DJI CS-SR1 UAV), and backbone is responsible for feature extraction. Through convolution and residual connections, image features are efficiently extracted to achieve the recognition and analysis of fault points in the image line. The YOLO series of target algorithms are all based on anchor box expansion for object detection [11]. Among them, the width and height of the anchor box are defined as p_w and p_n, and the offset of the X and Y axes in the upper left corner of the anchor diagram is set as c_x and c_y. When detecting the fault target point, the original anchor box is a dashed box, while the predicted box is a blue box. In the detection of power lines, the network needs to fine tune the anchor boxes based on four offsets t_y, t_x, t_h, and t_w to achieve accurate prediction of the results. The border prediction is in Eq. (1) [12].

$$\begin{cases} b_x = 2\sigma(t_x) - 0.5 + c_x \\ b_y = 2\sigma(t_y) - 0.5 + c_y \\ b_h = p_h(2\sigma(t_h))^2 \\ b_w = p_w(2\sigma(t_w))^2 \end{cases} \tag{1}$$

In Eq. (1), b_x, b_y, b_h, and b_w respectively represent the positions of the predicted border on the X and Y axes, as well as the height and width of the border, and σ represents the activation function. The principle of adjusting the anchor target box is in Fig. 2.

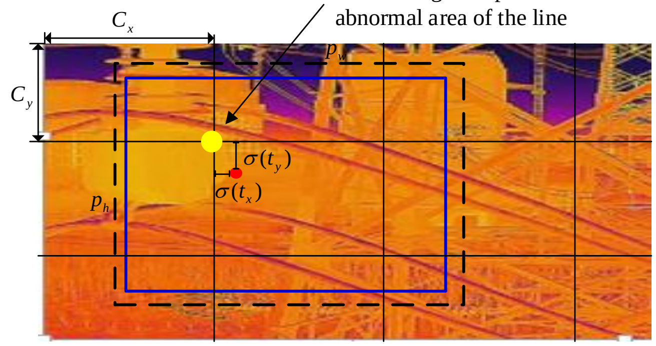

Fig. 2. Schematic diagram of anchor box target adjustment.

In Fig. 2, it is essential to adjust the parameters to make the prediction box detect the line fault point more accurately. However, in actual line fault detection, there are few fault points in aerial images. To enable the model to detect effective target points, the YOLOv5 bounding box (BB) regression function will be optimized to filter out useless anchor boxes and improve the detection efficiency of fault targets. The key area in Intersection over Union (IoU) is introduced to reflect the prediction of BB [13]. The loss function L_{IoU} for predicting similarity with the real border is calculated as presented in Eq. (2).

$$L_{IoU} = 1 - \frac{|A \cap B|}{|A \cup B|} \tag{2}$$

In Eq. (2), A represents the predicted anchor box and B denotes the real anchor box. In graph fault detection, if the IoU value is set to 1 and the anchor box is a positive sample, it indicates that the similarity between the predicted and real target anchor boxes is high, and both contain the target to be recognized. When the IoU value is below 0.5, the anchor boxes are negative samples and there is no intersection between the two anchor boxes. In addition, a loss function L_{GIoU} was introduced in the study to analyze the bounding rectangle of two anchor boxes. The analysis of bounding rectangles can better solve the proportion of non-overlapping areas, which is beneficial for determining the overlap distance between two anchor boxes [14]. The calculation of L_{GIoU} is in Eq. (3).

$$L_{GIoU} = 1 - IoU + \frac{|C - (A \cup B|}{|c|} \tag{3}$$

In addition, the study uses the d variable in the L_{DIoU} function to represent the Euclidean distance between the two center coordinates within the anchor box (points A and B), with a diagonal distance of c. The penalty term in the L_{DIoU} function can avoid the occurrence of larger BB when two anchor boxes are far apart, which affects the network's detection of fault points. The calculation of L_{DIoU} is in Eq. (4).

$$L_{DIoU} = 1 - 1oU + \frac{\gamma^2 (A_2 B)}{c^2} \tag{4}$$

In Eq. (4), γ represents the Euclidean distance parameter. In the L_{DIoU} function, if the loss value is large, L_{DIoU} is used for optimization, which is faster than the L_{DIoU} function, but it is not applicable when the midline points coincide. Therefore, by combining the Euclidean distance of the center point, overlapping area, and the aspect ratio of the border, a L_{CIou} function is introduced, which is expressed as Eq. (5).

$$L_{CIou} = 1 - loU + \frac{\gamma^2 (A, B)}{c^2} - av \tag{5}$$

In Eq. (5), a represents a comprehensive adjustment parameter and v represents the width height difference parameter. Although the L_{CIou} function can more accurately reflect the differences in anchor boxes, the width height difference parameter v cannot specifically reflect the differences in height and width between the real and predicted borders, making the optimization process of function L_{CIou} unreasonable. Therefore, the research has incorporated a focus on high-quality anchor box attention mechanism, namely $Loss_{EIoU}$ function, which enhances the screening of high-quality boxes based on function L_{CIou}, reducing the loss of width and height between the target box and anchor box [15]. Its expression is in Eq. (6).

$$L_{EIoU} = L_{IoU} + L_{dis} + L_{asp} = 1 - IoU + \frac{\lambda^2 (A, B)}{c^2} + \frac{\lambda^2 (w, w^{gt})}{c_w^2} + \frac{\lambda^2 (h, h^{gt})}{c_h^2} \tag{6}$$

In Eq. (6), w^{gt} and h^{gt} represent the disparities in anchor frame width and height, L_{asp} is the direction loss, c_w and c_h represent the highest value of coverage width and height, and L_{dis} is the distance loss. In addition, to enable the network to only detect high-quality line fault images, the study used IoU weighted processing to obtain the target loss function filtered by anchor boxes, as shown in Eq. (7):

$$L_{Focal-EIoU} = IoU^{\ell} L_{EIoU} \tag{7}$$

In Eq. (7), ℓ represents the suppression quality sample parameter in the network. In this research section, the improvement of the anchor box part in YOLOv5 enhances the network's screening and recognition of fault samples in line images, improving the efficiency and quality of network detection.

B. Line Fault Detection Modeling Based on YOLOv5 and DT Model

In the previous section, the improved YOLOv5 algorithm was used to detect line faults. However, in large-scale multi-objective power networks, this technology cannot quickly achieve efficient detection of multiple faulty lines, limiting its applicability. Therefore, the next step is to introduce DT technology to determine large-scale line fault points, while utilizing the improved YOLOv5 algorithm to achieve efficient detection of multi-target fault points. Among them, the power DT model is in Fig. 3.

According to Fig. 3, the power DT model contains two main parts: the physical power grid and the virtual power grid. Among them, the physical part includes temperature, wind speed, visual detection, and other sensor parts, responsible for detecting the status of power grid transformers, lines, and various equipments in real scenes. The virtual part will map physical entity data to the geometric model of the power grid, and feedback the state information to the application layer through the twin data center, thereby achieving real-time monitoring of the power network [16]. Therefore, the study utilizes twin models to quickly determine the location of power line faults, while adopting an improved YOLOv5 algorithm to achieve rapid detection of multi-objective fault points. One notable aspect is that, within the DT model, it is of paramount importance to dynamically map physical spatial data onto the virtual space. This dynamic mapping is governed by the equation presented in Eq. (8).

$$G_v(t) = \Phi(G_p(t), \Theta) + \grave{o}(t)\Theta = \{T(t), W(t), V(t)\} \tag{8}$$

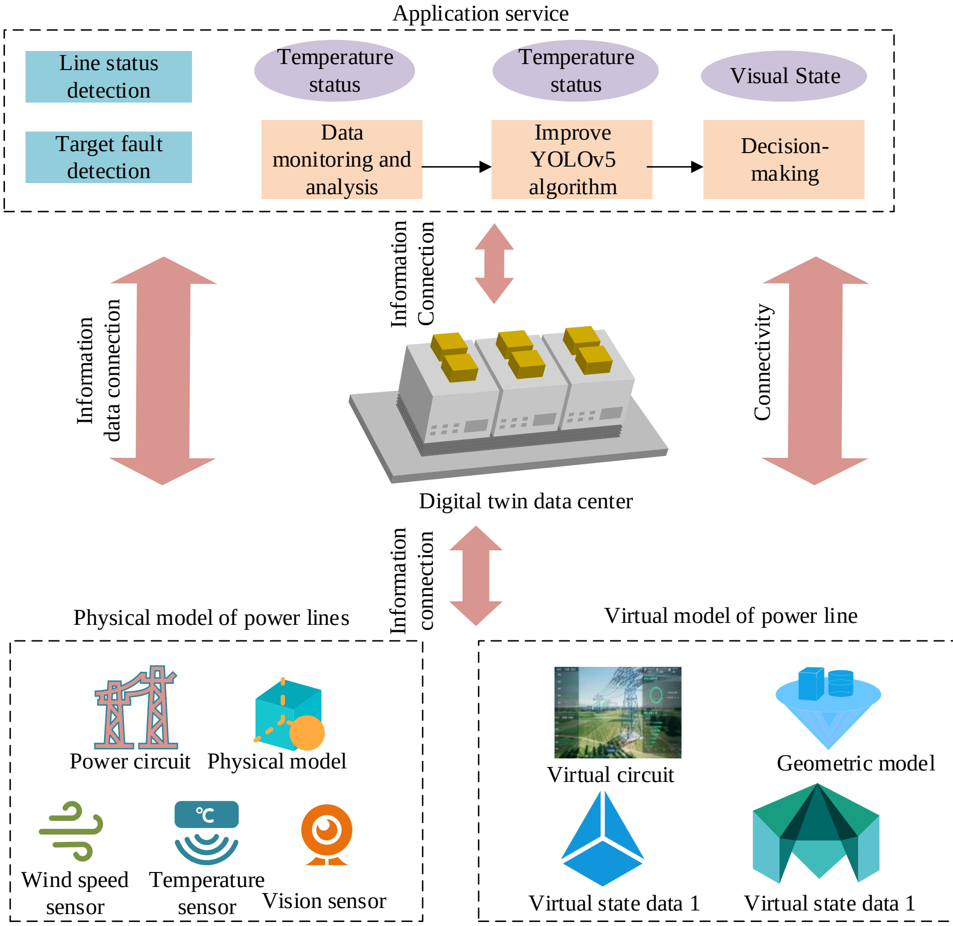

Fig. 3. Diagrammatic representation of power DT model.

In Eq. (8), $G_p(t)$ represents the physical power grid line state, $T(t)$ is the temperature state model, $W(t)$ is the wind speed state model, and $V(t)$ is the visual feature state model. $\Phi(\cdot)$ is a dynamic encoder based on Long Short-Term Memory (LSTM) network. Θ is the set of environmental parameters. $\grave{o}(t)$ is the Gaussian noise parameter. Next, through the monitoring data of the physical model, an anomaly detection mechanism is established in the virtual space to achieve rapid localization of the fault area. The localization equation is in Eq. (9).

$$F_{region} = \arg\max_{x,y}\left[\| H_t(x,y)-H_{t-1}(x,y)\|_2^2 \cdot S_{thermal}(x,y)\right] \quad (9)$$

In Eq. (9), H_t is the thermal distribution matrix of the power grid at time t. $S_{thermal}$ is the weight matrix for temperature anomalies. (x, y) is the coordinate system for the fault point. After determining the location of power line faults that need to be detected in the power grid system, the improved YOLOv5 algorithm is adopted as a multi-objective fault detection technique. Firstly, to enhance the training swiftness of the network and reduce the number of parameters, GhostNet is used to replace the Conv module and CSP Bottleneck with three convolutions (C3) in the YOLOv5 backbone network. The GhostNet structure is in Fig. 4 [17].

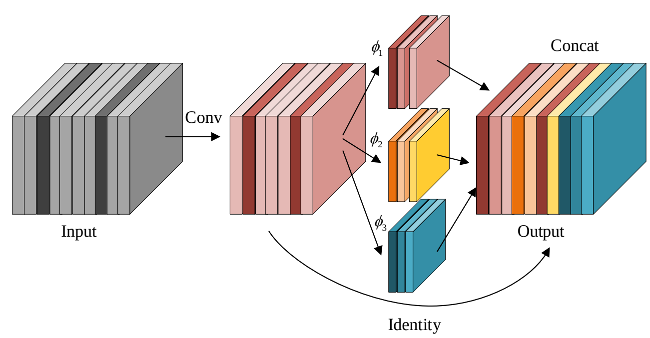

Fig. 4. GhostNet structure.

In Fig. 4, compared to the Conv module and C3 module in the traditional YOLOv5 backbone network, the GhostNet divides convolution into two processes: Identity operation and Concat operation, including using a small number of convolution operations first, followed by stepwise channel convolution operation. The output of the GhostNet is in Eq. (10).

$$Y = [X \# W_1, \phi(X \# W_2)] \tag{10}$$

In Eq. (10), $\#$ represents the convolution operation, and $\phi(\cdot)$ is depthwise separable convolution. X is the input feature map. W_1 and W_2 represent the corresponding weights of standard convolution and depthwise separable convolution, respectively. In GhostNet feature extraction, the channel compression ratio is set to 1:3. Next, to better adaptively analyze the sudden changes in lighting and hotspots in the power grid, an adaptive activation function, Activate Or Not (ACON), was studied to replace the original Leaky ReLU function, which can dynamically adjust the activation threshold. The calculation of the activation function is in Eq. (11) [18].

$$ACON(x) = (p_1 - p_2)x \cdot \sigma(\beta x) + p_2 x \tag{11}$$

In Eq. (11), p_1 and p_2 are both trainable parameters. β is the adaptive adjustment activation threshold. σ is the activation function. In addition, in multi-target power line fault detection, including scenes such as forests and buildings, the images extracted by UAVs contain complex background information, making it difficult to locate line faults such as insulator breakage and wire wear. Therefore, the study introduces a CA mechanism between the backbone network and the feature pyramid to enhance the extraction of key features in images. The process of changes in CA mechanism is in Eq. (12) [19].

$$\begin{cases} z_c = \dfrac{1}{H \times W} \sum_{i=1}^{H} \sum_{j=1}^{W} x_c(i, j) \\ m = f^{1\times1}([z^h, z^w]) \\ g = \sigma(Conv([AvgPool_h(x), AvgPool_w(x)])) \end{cases} \tag{12}$$

In Eq. (12), z_c represents the input of channel information and x_c represents the corresponding channel information input. m represents the location information of the region of interest processed by the 1×1 convolutional transformation function f. z^h and z^w respectively represent the height and width of the position of interest. H and W represent the height and width of the feature map. $AvgPool$ represents global average pooling. g represents spatial attention weight. The output of the CA machine is in Eq. (13).

$$y = X \cdot m \cdot g \tag{13}$$

In Eq. (13), X represents the given input feature information. In addition, to enhance the infrared imaging features and small target features, such as detecting loose bolts and other targets, the study used Bidirectional Feature Pyramid Network (BiFPN) to replace the original path aggregation network structure, and its weighted fusion expression is in Eq. (14) [20].

$$P_l^{out} = \sum_i \frac{w_i}{\epsilon + \sum_j w_j} \cdot Resize(P_i^{in}) \tag{14}$$

In Eq. (14), w_i is the learnable weight parameter. P_i^{in} represents the input features of the i th level, which are composed of multiple features together. $Resize(\cdot)$ represents feature size alignment operation. ϵ represents the minimum constant. w_j represents fusion weight. Finally, based on the above analysis, the end-to-end joint line fault detection results are obtained, as shown in Eq. (15) [21].

$$\begin{cases} \mathrm{F} = BiFPN(GhostNet(I_{512\times512})) \\ \mathrm{D} = \bigcup_{k=1}^{4} \{(x, y, w, h, cls) \mid conf_k > 0.5\} \\ conf_k = \prod_{m=1}^{3} CA_m(ACON(\mathrm{F}_k)) \end{cases} \tag{15}$$

In Eq. (15), F represents the multi-scale feature pyramid processed by GhostNet and BiFPN. D represents the final set of detection results, where cls represents the category, (x, y, w, h) represents the BB coordinates, and k represents the corresponding four detection heads, namely P_1, P_2, P_3, and P_4. $conf_k$ represents the confidence level of the detection head, which is weighted and calculated through the CA attention module. I represents the fault area image provided by the DT system. Finally, the study adopted an improved k-loss function as the prediction output, and the results are shown in Eq. (16).

$$\mathrm{L} = \lambda_{box}(1 - IoU)^{\delta} + \lambda_{cls} FL(p_t) + \lambda_{obj} BCE(\hat{o}, o) \tag{16}$$

In Eq. (16), λ_{box}, λ_{box}, and λ_{obj} represent the weight coefficients of BB loss, classification box loss, and target confidence loss, respectively. δ is the focusing factor, which reduces the loss contribution of simple samples and focuses on difficult samples. $FL(p_t)$ is the classification loss, and p_t represents the probability of model category prediction. $BCE(\hat{o}, o)$ is the confidence loss, where o is 0 indicating that the target is the background, 1 indicating that the target exists, and $\hat{o}$ is the confidence of the model target. The entire technical process is in Fig. 5.

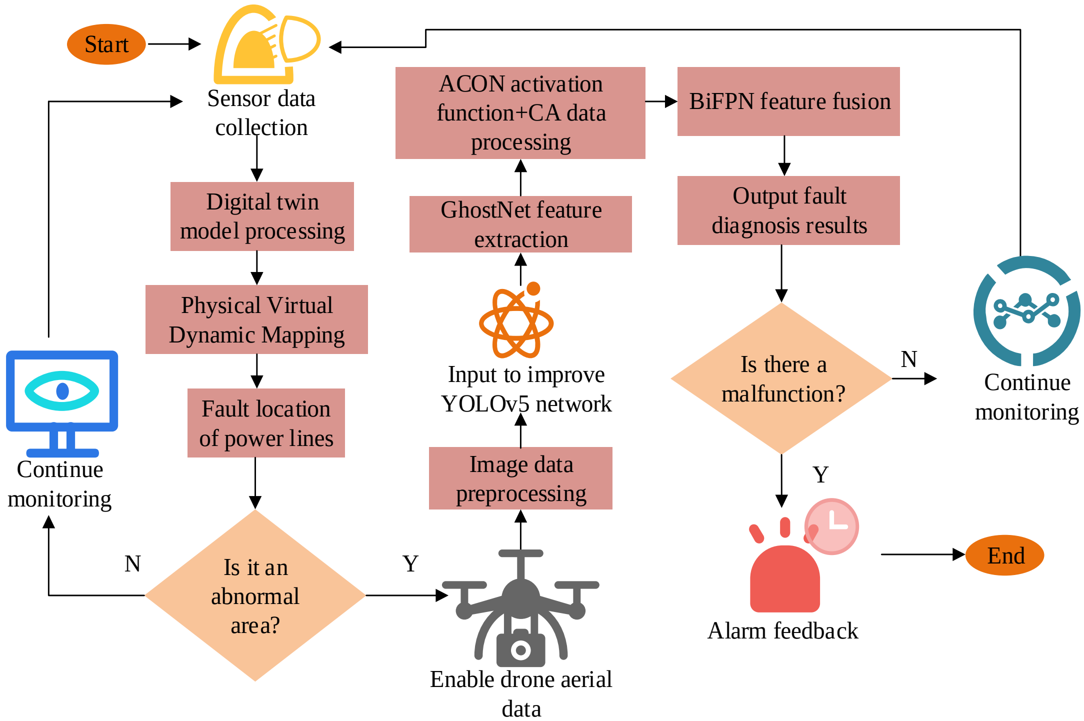

Fig. 5. Line fault diagnosis based on improved YOLOv5 and DT model.

Fig. 5 shows the process of fault diagnosis for power lines, in which a DT model is used to analyze the external environment of the power grid line and identify the location of the line fault point. Secondly, by using UAVs to obtain image information of fault line points, and improving the YOLOv5 algorithm training, the detection of multi-target point faults in power lines can be achieved.

IV. RESULTS

A. *YOLOv5 BB Regression Loss Function Performance Experiment*

To test the application effect of the power fault diagnosis technology proposed by the research in practical scenarios, corresponding experimental analysis was carried out next. The training was conducted using Python version 3.8 and the DL framework was PyTorch. The training parameter settings of the improved YOLOv5 model was presented in Table I.

Comprehensive and Special Data (CSD) and self-made datasets were selected for the experiment. The CSD dataset includes UAV inspection images, wire and conductor loose strand detection datasets, and infrared image insulator detection datasets. It supports YOLO analysis format and has a total of about 30000 images. Meanwhile, the study used DJI CS-SR1 (visible light+infrared dual-mode) to capture a total of 27200 images of power lines, labeled in YOLO format, with an image size of 1024×1024. It covers data from different seasons, backgrounds, and lighting conditions. Next, the study investigated the anchor box performance of various optimized loss functions tested on the CSD dataset, where the default IoU function and Focal EIoU function were not used. In the anchor box, Focal EIoU is consistent with EIoU, as presented in Fig. 6.

In Fig. 6, GIoU, CIoU, and EIoU loss functions were selected for testing in the study. At 10 iterations, all three loss functions were located at the anchor box position and remained basically consistent. After 150 iterations, the three loss functions showed significant differences, among which the GIoU function, although able to match the target box, covered both the target box and anchor box with average accuracy. The CIoU function outperformed GIoU in matching performance and could cover the target box more accurately, but the target box repetition was still relatively low. The best matching function was the EIoU function, which basically covered the target box completely and achieved an accuracy of 98.58%, showing the best performance. Next, the study compared the regression loss and IoU performance of five types of losses, as presented in Fig. 7.

TABLE I. MODEL PARAMETER SETTINGS

Model indicators	Parameter
Image size	1024x1024
Batch size	16
Initial learning rate	1e-3
Anchor frame size	[12, 16], [20, 28], [24, 36], [36, 48], [48, 64]
Boundary box loss box	4.8
Classification loss CLS	8.5
Number of iterations	200

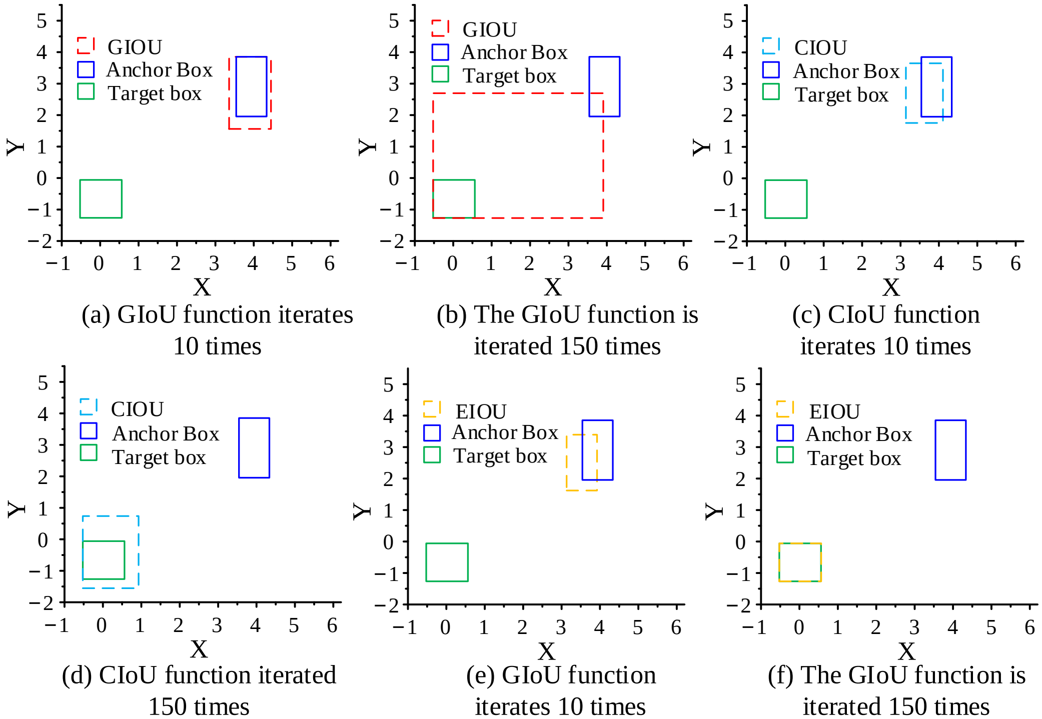

(a) GIoU function iterates 10 times
(b) The GIoU function is iterated 150 times
(c) CIoU function iterates 10 times
(d) CIoU function iterated 150 times
(e) GIoU function iterates 10 times
(f) The GIoU function is iterated 150 times

Fig. 6. Anchor box performance of different loss functions at 10 and 150 iterations.

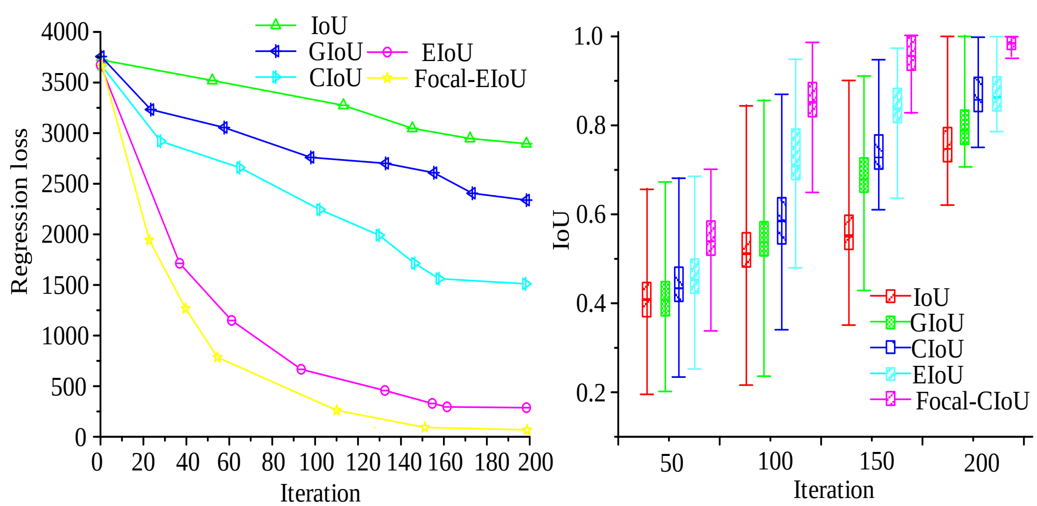

(a) Regression loss of different loss functions
(b) Intersection over union ratio of different loss functions

Fig. 7. Comparison of regression loss and IoU ratio with different loss functions.

Fig. 7 indicates the comparison results of function regression losses. According to the test results, the five loss functions showed different performance during training. Among them, EIoU and Focal EIoU functions converged the best, and thanked to filtering the anchor boxes, Focal EIoU had the best regression loss performance, with a regression loss of 125 and EIoU function of 256 during convergence. Fig. 7(b) indicates the test results of the IoU ratio of different loss functions, whose values reflect the accuracy of BB matching. The higher the value, the greater the intersection between the anchor box and the target box. According to the test results, as the iteration count increased, the IOU values of the five loss functions gradually increased, and the optimal IOU value was obtained after 200 iterations. Among them, the best performing Focal EIoU had a mean of 0.986 and a minimum value of 0.956, followed by EIoU with a mean of 0.926 and a minimum value of 0.796. The overall performance of other loss functions was average, although the maximum IOU value could reach 100%, the mean and minimum values were relatively low. Next, the study selected the self-made data nest scene for detection and determined the confidence values of different loss functions, as presented in Fig. 8.

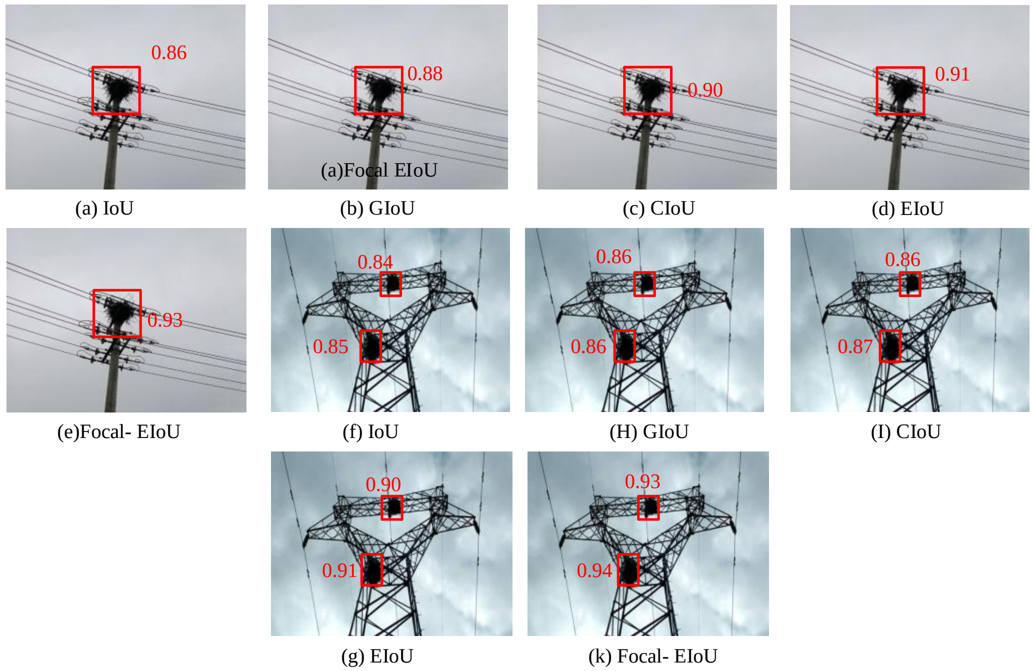

Fig. 8. Confidence level of object detection with various loss functions.

In Fig. 8, the selected route had a bird's nest scene for object detection. Among them, Fig. 8(a) to Fig. 8(e) are scene 1. In this scenario, the highest confidence level among the five loss functions was Focal IoU, which was 0.93. Next was EIoU, with a confidence level of 0.91, while CIoU, GIoU, and IOU had confidence levels of 0.90, 0.88, and 0.86, respectively. Figs. 8(f) to 8(k) show scene 2, which included two types of bird nests: large and small targets. Focal IoU performed the best overall, with confidence levels of 0.93 and 0.94, indicating the best performance.

B. Multi-Scenario Fault Detection Test for Power Lines

Next, Focal IoU was chosen as the loss function for the recognition model, and Faster R-CNN and YOLOv7 were introduced as testing benchmarks to compare their performance in detecting power line faults. Among them, the standard dataset CSD was selected for testing to compare the training accuracy and loss of different models, as presented in Fig. 9.

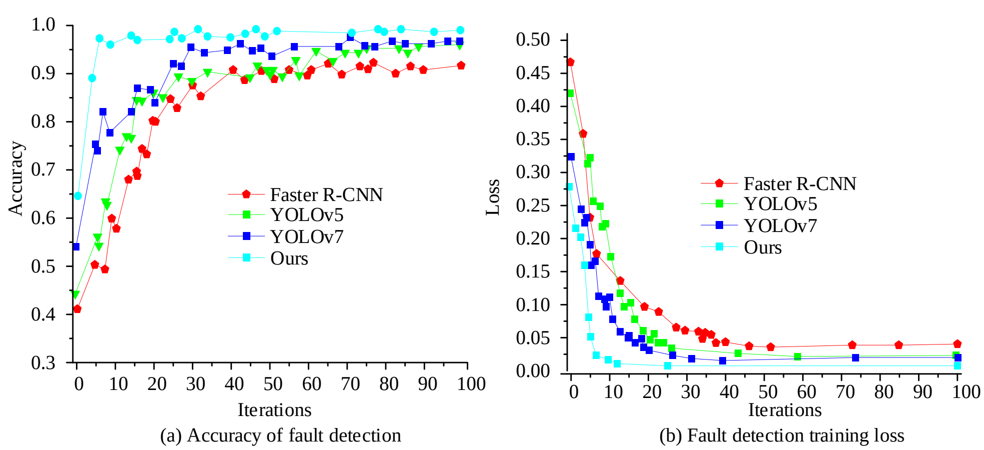

Fig. 9. Fault detection performance of different models.

Fig. 9(a) indicates the accuracy of fault detection. Among the four models, the research model achieved the fastest convergence with a maximum accuracy of 0.986, followed by YOLOv7 with a convergence of 0.95. YOLOv5 and Faster R-CNN performed average, with convergence accuracies of 0.948 and 0.902. Fig. 9(b) indicates the training loss results of different models. Among them, the Faster R-CNN table had a general convergence loss of 0.051. YOLOv5 performed similarly to YOLOv7, but YOLOv7 had better convergence with loss values of 0.025 and 0.024. The research model performed the best, with a convergence loss value of 0.0125. Next, the study selected different scenarios from the self-made dataset to compare the accuracy of technical fault diagnosis, as shown in Fig. 10.

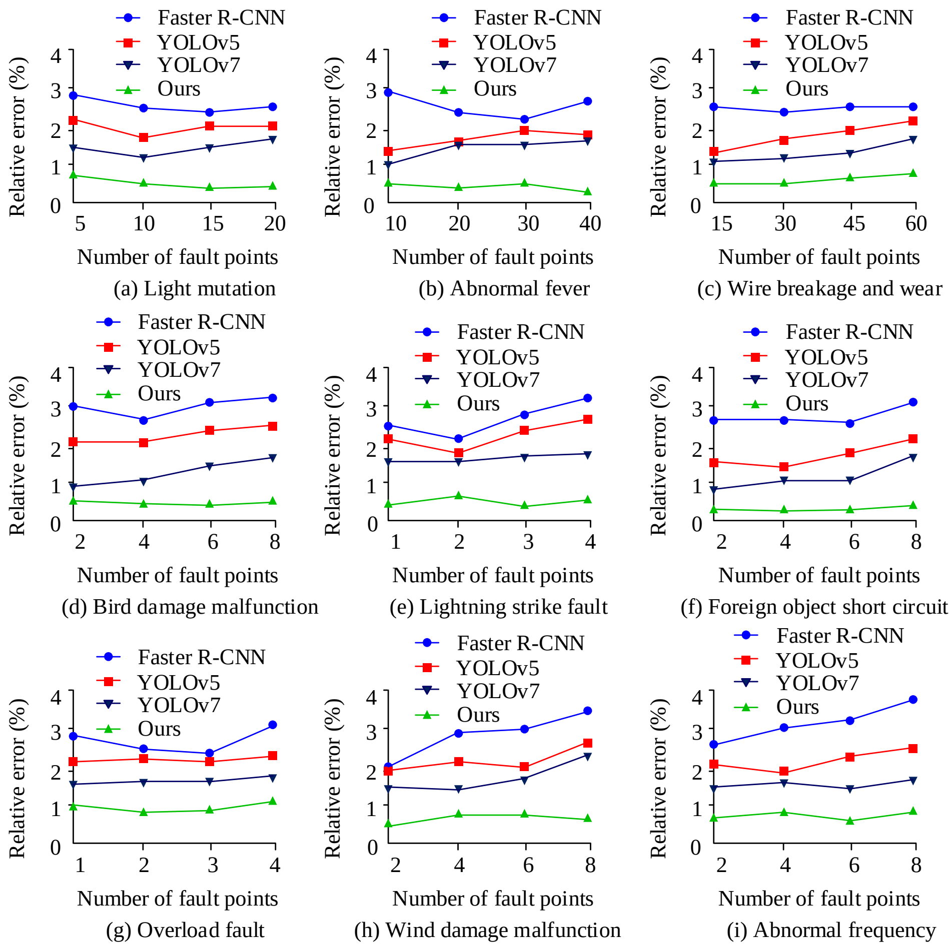

Fig. 10. Multi-scenario line fault diagnosis accuracy.

In Fig. 10, nine common circuit faults were selected for detection, including sudden changes in infrared scene lighting, abnormal light emission, etc. According to the test results, an increase in target data had a certain impact on the accuracy of model detection. Among them, the research model performed the best, with a relative error controlled within 1.2% in nine scenarios. Secondly, YOLOv7 had a relative error controlled within 2.7%. However, YOLOv5 and Faster R-CNN had significant overall detection errors. When the number of targets reached four in abnormal heat detection, the errors of all four models increased, but the relative error of the research model was the lowest at 0.86%, while YOLOv7 was 1.89%, and YOLOv5 and Faster R-CNN were 2.86% and 3.35%, respectively. Finally, the recognition frame rate and diagnostic time were tested on the self-made dataset, as presented in Fig. 11.

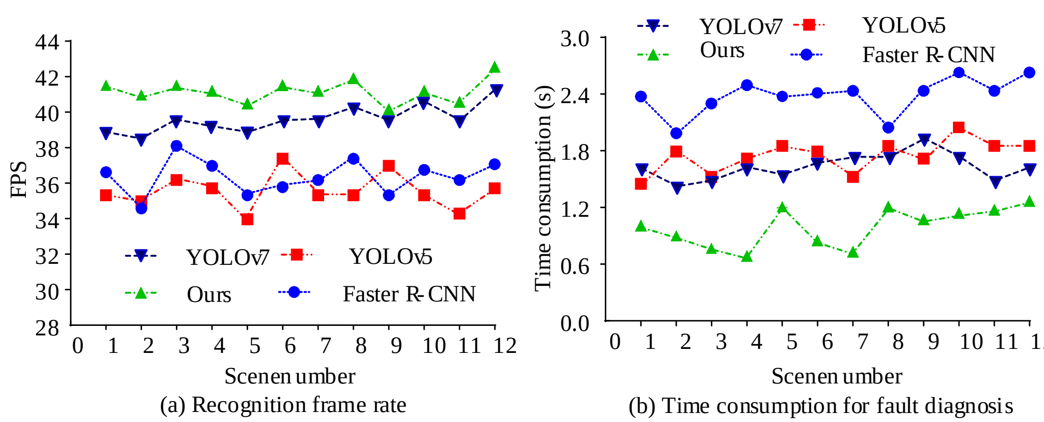

Fig. 11. Recognition frame rate and diagnosis time.

Fig. 11(a) indicates the results of the frame rate recognition test. Selected twelve fault scenarios for testing. The average frame rates of the research model, YOLOv7, YOLOv5, and Faster R-CNN were 41.2 frames, 39.5 frames, 35.8 frames, and 37.86 frames, respectively. Fig. 11(b) shows the time-consuming results of fault diagnosis, among which Faster R-CNN performed the worst, taking over 1.8 seconds in multiple scenarios, with an average time of 2.05 seconds. YOLOv7 and YOLOv5 performed better, with average fault diagnosis times of 18.95 seconds and 18.64 seconds, respectively. The best performing model was the research model, with an average fault diagnosis time of 10.25 seconds. Finally, the study selected ten types of power line faults in real scenarios for on-site experimental analysis to test the detection effectiveness of four techniques for different line fault problems. The test results are shown in Table II.

TABLE II. COMPARISON OF LINE FAULT DETECTION EFFECTS OF DIFFERENT TECHNOLOGIES IN REAL SCENARIOS

Line fault type	**10 rounds of testing for fault detection accuracy**			
	Faster R-CNN	**YOLOv5**	**YOLOv7**	**Ours**
Damaged insulator	90	90	100	100
Wire breakage	70	90	90	100
Loose fittings	40	50	70	100
Corrosion of anti vibration hammer	70	70	80	100
Bird's Nest Construction	90	90	100	100
Foreign object suspension	90	100	100	100
Tower tilt	70	80	100	100
Insulator self explosion	50	60	70	100
Wire wear and tear	90	90	90	100
Deformation of metal fittings	60	70	80	100

Table II shows the test results of different line faults in real scenarios. According to the test results, all four diagnostic models for conventional fault types could effectively diagnose, such as insulator damage and wire wear during bird nest construction. However, for fault types with small targets and complex backgrounds, except for the research model that could recognize 100%, all other models performed average. In the detection of loose fittings, the accuracy of Faster R-CNN was 40%, while YOLOv5 and YOLOv7 were 50% and 70%, respectively. Only the research model achieved 100% in ten tests. In addition, in the summary of insulator self explosion detection, Faster R-CNN, YOLOv5, YOLOv7, and research model detection accuracies were 50%, 60%, 70%, and 100%, respectively. In practical scene detection, the research technology performed excellently.

V. DISCUSSION

Ensuring the secure and dependable functioning of power grid lines is essential for reliable power supply. Traditional detection methods rely on manual inspection, which suffers from issues like inefficiency and poor real-time performance. The rise of DL technology and DT technology provides new avenues for power grid line detection. To address these issues, a power line fault detection technique combining DL and DT models is raised.

In the experiment, an improved YOLOv5 model was adopted and its anchor box loss function was optimized. Experimental data showed that the improved Focal IoU loss function performed well in terms of regression loss and IoU. Specifically, the regression loss value of Focal IoU was 125, and the mean IoU was 0.986, which was significantly better than other loss functions. In addition, the study introduced GhostNet and CA mechanism, further improving the detection capability of the model in complex scenes. The GhostNet reduced the number of parameters and improves training speed by dividing convolution into two processes: Identity operation and Concat. The CA mechanism enhanced the extraction of key features in images and improved the detection accuracy of the model in complex backgrounds. In multi-scenario fault detection, the accuracy of the research model reached 0.986, with a loss value of 0.0125, which was superior to models such as Faster R-CNN and YOLOv7. By comparison, Faster R-CNN was a two-stage detector that first generated region proposals, and then classified and regressed each proposal, resulting in higher computational complexity and poorer real-time performance [22]. Although YOLOv7 performed well in real-time, there is still room for improvement in detection accuracy when dealing with small targets [23]. Especially in complex background environments, there were issues such as detection omissions and errors, which resulted in lower overall accuracy compared to the improved YOLOv5. For example, in abnormal heat detection, when the number of targets was four, the relative error of the research model was only 0.86%, while the errors of other models were all higher than 1.89%. These results indicated that the improved YOLOv5 model combined with DT technology could effectively improve the accuracy and efficiency of power line fault detection.

In addition, the research technology system also had excellent security and stability. Especially in the analysis and detection of power lines, DL and twinning techniques were utilized. To ensure that power data was not attacked and to avoid data leakage, the Advanced Encryption Standard (AES) was introduced in the research to encrypt all transmitted data, ensuring the confidentiality and integrity of the data during transmission [24]. In addition, potential external information attacks such as Denial of Service (DoS) and Distributed Denial of Service (DDoS) [25] should be addressed. In addition, from a hardware perspective, the research adopted the latest 64 bit ARM encryption processor, which had strong environmental adaptability and security, thus ensuring the effectiveness of the entire technology [26].

Overall, the improvement of YOLOv5 was more effective than YOLOv5 in power line fault diagnosis. Especially in complex and small target scenarios, the technology proposed by the research had higher overall accuracy, stronger adaptability, and better met the requirements of fault detection in power scenarios. In addition, the combination of research technology and DT technology further enhanced the application effect of technology in power scenarios, and provided important technical support for the construction and management of power informationization.

VI. CONCLUSION

The safe and stable operation of power grid lines is crucial for power supply. Traditional detection methods rely on manual inspection, which has problems such as low efficiency and poor real-time performance. To solve the above problems, the research proposed an intelligent line fault detection technology based on improved YOLOv5. Firstly, the research optimized the BB regression loss function of YOLOv5 by introducing the Focal IoU loss function to filter out useless anchor boxes and improve the detection efficiency of fault targets. Secondly, the introduction of GhostNet network and CA attention mechanism further enhanced the diagnostic performance of YOLOv5 in complex scenes. In addition, the research also combined DT technology to construct virtual models and map physical entity states in real time, achieving accurate monitoring and fault warning of power equipment. The experimental results showed that the improved YOLOv5 model outperformed other loss functions in terms of BB regression loss and intersection to union ratio performance. The Focal IoU function had the lowest regression loss value and the highest average intersection to union ratio. In multi-scenario fault detection of power lines, the average accuracy of the improved model reached 98.6%, significantly higher than other models. Under the self-made dataset, the average fault diagnosis time of the improved model was 10.25 seconds, which was much lower than other models. From this, the intelligent line fault diagnosis technology proposed by the research, which combined the DT model with the improved YOLOv5 algorithm, could effectively improve the accuracy and real-time performance of power line fault detection. The research significantly improved the performance of power line fault detection by improving the YOLOv5 model. However, there are still some shortcomings in this study. For example, the adaptability of the model under extreme weather conditions needs further validation. In addition, researching how to use drones to obtain images to improve the perspective of drone image extraction is the key to diagnosis. Therefore, in future work, research needs to be conducted from three aspects. 1) To improve the effectiveness of technology, it is necessary to enhance its adaptability to complex environments and optimize the process of drone image recognition. 2) Meanwhile, in future work research, the fusion analysis of multi-scale features can be considered to enhance the detection of complex backgrounds and small targets through technology. 3) In addition, the study also strengthened the integration of DTs and DL, for example, using virtual data generated by DT models to enhance the training dataset, improve the model's generalization ability, and optimize model training and updates through real-time feedback of fault diagnosis results from DT models.

REFERENCES

[1] M. Khaleel, S. A. Abulifa, and A. A. Abulifa, “Artificial intelligent techniques for identifying the cause of disturbances in the power grid,” Brilliance: Research of Artificial Intelligence, vol. 3, no. 1, pp. 19-31, February 2023.

[2] S. Rangarajan, R. Raman, A. Singh, and C. K. Shiva, “DC microgrids: a propitious smart grid paradigm for smart cities,” Smart Cities, vol. 6, no. 4, pp. 1690-1718, March 2023.

[3] A. Stonier, R. Harish, and M. Srinivasan, “An extensive critique on fault-tolerant systems and diagnostic techniques intended for solar photovoltaic power generation,” ENERG SOURCE PART A, vol. 45, no. 1, pp. 1856-1873, June 2023.

[4] F. M. Shakiba, S. M. Azizi, M. Zhou, and A. Abusorah, “Application of machine learning methods in fault detection and classification of power transmission lines: a survey,” ARTIF INTELL REV, vol. 56, no. 7, pp. 5799-5836, July 2023.

[5] Z. Li, Y. Zhang, H. Wu, S. Suzuki, and A. Namiki, “Design and application of a UAV autonomous inspection system for high-voltage power transmission lines,” REMOTE SENS-BASEL, vol. 15, no. 3, pp. 865-872, August 2023.

[6] Y. Chen, Y. Wang, X. Tang, S. Wu, and R. Guo, “Intelligent power distribution live-line operation robot systems based on stereo camera,” High Voltage, vol. 8, no. 6, pp. 1306-1318, September 2023.

[7] E. Gómez-Luna, J. E. Candelo-Becerra, and J. C. Vasquez, “A new digital twins-based overcurrent protection scheme for distributed energy resources integrated distribution networks,” ENERGIES, vol. 16, no. 14, pp. 5545-5561, October 2023.

[8] M. Sinagra, E. Creaco, G. Morreale, and T. Tucciarelli, “Energy recovery optimization by means of a turbine in a pressure regulation node of a real water network through a data-driven digital twin,” WATER RESOUR MANAGt, vol. 37, no. 12, pp. 4733-4749, November 2023.

[9] A. Sharma and M. Kumar Tiwari, “Digital twin design and analytics for scaling up electric vehicle battery production using robots,” International Journal of Production Research, vol. 61, no. 24, pp. 512-8546, December 2023.

[10] W. Hu, T. Wang, and F. Chu, “Novel Ramanujan digital twin for motor periodic fault monitoring and detection,” IEEE T IND INFORM, vol. 19, no. 12, pp. 11564-11572, January 2023.

[11] D. E. A. Mansour, M. Numair, A. S. Zalhaf, R. Ramadan, M. Darwish, and M. Hussien, “Applications of IoT and digital twin in electrical power systems: A comprehensive survey,” IET GENER TRANSM DIS, vol. 17, no. 20, pp. 4457-4479, February 2023.

[12] P. Palensky, P. Mancarella, and T. Hardy, “Cosimulating integrated energy systems with heterogeneous digital twins: matching a connected world,”IEEE POWER ENERGY M, vol. 22, no. 1, pp. 52-60, March 2024.

[13] N. Singh, M. A. Ansari, and M. Tripathy, “Feature extraction and classification techniques for power quality disturbances in distributed generation: a review,” IETE J RES, vol. 69, no. 6, pp. 3836-3851, April 2023.

[14] Z. Li, K. Liu, M. Lin, D. Xing, H. Tang, and G. Wu, “A zero-sample state evaluation model for valve-side bushing of UHV converter oriented to digital twin under attribute analysis,” IET GENER TRANSM DIS, vol. 17, no. 5, pp. 1123-1134, May 2023.

[15] S. Alam, “Characterizing the data landscape for digital twin integration in smart cities,” Journal of Intelligent Connectivity and Emerging Technologies, vol. 8, no. 4, pp. 27-44, June 2023.

[16] Y. Kim, S. Hakak, and A. Ghorbani, “Smart grid security: attacks and defence techniques,” IET Smart Grid, vol. 6, no. 2, pp. 103-123, July 2023.

[17] E. Badakhshan and P. Ball, “Deploying hybrid modelling to support the development of a digital twin for supply chain master planning under disruptions,” INT J PROD RES, vol. 62, no. 10, pp. 3606-3637, August 2024.

[18] [M. Dellaly, S. Skander-Mustapha, and I. Slama-Belkhodja, “A digital twin model-based approach to cost optimization of residential community microgrids,” Global Energy Interconnection, vol. 7, no. 1, pp. 82-93, September 2024.

[19] N. Chinthamu and M. Karukuri, “Data science and applications,” Journal of Data Science and Intelligent Systems, vol. 1, no. 1, pp. 83-91, October 2023.

[20] A. Mohammad-Alikhani, B. Nahid-Mobarakeh, and M. F. Hsieh, “One-dimensional LSTM-regulated deep residual network for data-driven fault detectio in electric machines,” IEEE T IND ELECTRON, vol. 71, no. 3, pp. 3083-3092, November 2023.

[21] T. Mian, A. Choudhary, and S. Fatima, “Multi-sensor fault diagnosis for misalignment and unbalance detection using machine learning,” IEEE T IND APPL, vol. 59, no. 5, pp. 5749-5759, December 2023.

[22] P. Sanal, E. Karagoz, H. Seo, R. Azarderakhsh, and M. Mozaffari-Kermani, “Kyber on ARM64: Compact implementations of Kyber on 64-bit ARM Cortex-A processors,” in Proc. International Conference on

Security and Privacy in Communication Systems, Cham, Springer International Publishing, 2021, pp. 424-440, January 2021.

[23] B. Koziel, R. Azarderakhsh, and M. M. Kermani, “A high-performance and scalable hardware architecture for isogeny-based cryptography,” IEEE T COMPUT, vol. 67, no. 11, pp. 1594-1609, February 2018.

[24] M. Bisheh-Niasar, R. Azarderakhsh, and M. Mozaffari-Kermani, “Instruction-set accelerated implementation of CRYSTALS-Kyber,” IEEE T BIOMED CIRC S: Regular Papers, vol. 68, no. 11, pp. 4648-4659, March 2021.

[25] R. Azarderakhsh, K. U. Järvinen, and M. Mozaffari-Kermani, “Efficient algorithm and architecture for elliptic curve cryptography for extremely constrained secure applications,” IEEE Transactions on Circuits and Systems I: Regular Papers, vol. 61, no. 4, pp. 1144-1155, April 2014.

[26] A. Jalali, R. Azarderakhsh, and M. M. Kermani, “Supersingular isogeny Diffie-Hellman key exchange on 64-bit ARM,” IEEE T CIRCUITS-I, vol. 16, no. 5, pp. 902-912, May 2017.